Acta Crystallographica Section D
Biological Crystallography
ISSN 0907-4449

Preparation, crystallization and preliminary X-ray analysis of a complex between the *Plasmodium vivax* sexual stage 25 kDa protein Pvs25 and a malaria transmission-blocking antibody Fab fragment

Ajay K. Saxena,[a] Kavita Singh,[a] Carole A. Long[b] and David N. Garboczi[a]*

[a]Structural Biology Section, Laboratory of Immunogenetics, National Institute of Allergy and Infectious Diseases, National Institutes of Health, Twinbrook II, 12441 Parklawn Drive, Rockville, Maryland 20852, USA, and [b]Malaria Vaccine Development Branch, National Institute of Allergy and Infectious Diseases, National Institutes of Health, Twinbrook I, 5640 Fishers Lane, Rockville, Maryland 20852, USA

Correspondence e-mail: dgarboczi@niaid.nih.gov

Received 22 July 2004
Accepted 1 September 2004

The *Plasmodium vivax* sexual stage 25 kDa protein Pvs25, located on the surface of the ookinete form of the parasite, is a vaccine candidate designed to elicit immunity that blocks the transmission of malaria by mosquitoes. The 2A8 murine monoclonal antibody directed against recombinant Pvs25 prevents the formation of *P. vivax* oocysts in mosquitoes fed in the laboratory. The complex between recombinant Pvs25 and the Fab fragment of 2A8 forms crystals that diffract X-rays to 3.5 Å. Two native data sets, *A* and *B*, have been collected from crystals of the Pvs25–Fab complex. Both crystals belong to space group $P2_1$, with unit-cell parameters of $a = 86.3$, $b = 61.7$, $c = 142.7$ Å, $\beta = 101.7^\circ$ for data set *A* and $a = 86.8$, $b = 61.0$, $c = 149.3$ Å, $\beta = 104.3^\circ$ for data set *B*, and contain two complex molecules per asymmetric unit. Efforts are under way to reveal the structure of the Pvs25–Fab complex by molecular replacement. The three-dimensional structure of the Pvs25–Fab complex will provide an understanding of the interaction between Pvs25 and the 2A8 antibody that inhibits ookinete development in the mosquito and should aid in the development of transmission-blocking vaccines against *P. vivax* malaria.

1. Introduction

Malaria arises from the infection of red blood cells by protozoan parasites of the genus *Plasmodium* and is transmitted by anopheline mosquitoes. Four species of malaria parasites infect humans: *P. falciparum*, *P. vivax*, *P. ovale* and *P. malariae*. While *P. falciparum* is responsible for most of the mortality, *P. vivax* also causes high morbidity for millions of people in tropical and subtropical countries mainly outside sub-Saharan Africa (Mendis *et al.*, 2001).

Transmission-blocking vaccines using antigens that are expressed at the surface of the parasite sexual and mosquito stages, *i.e.* gametocytes, gametes, zygotes and ookinetes, are promising strategies for malaria control (for a review, see Stowers & Carter, 2001). Two examples of such antigens are the ookinete surface proteins of *P. vivax*, Pvs25 and Pvs28. Pvs25 and Pvs28 proteins exhibit structural characteristics of a family of proteins from *Plasmodium* parasites, consisting of a signal sequence at the N-terminus, four tandem epidermal growth-factor-like domains and a C-terminal glycosyl-phosphatidyl-inositol moiety anchoring the protein to the parasite surface. Homologous proteins have been cloned from several species of malaria parasites that infect humans (Kaslow *et al.*, 1988; Tsuboi *et al.*, 1998; Tachibana *et al.*, 2001) and from several species that infect animals.

Transmission-blocking vaccines induce antibodies which are taken up by a mosquito during blood feeding from the vertebrate host. In the mosquito midgut, the antibodies inhibit parasite development and thus block parasite transmission from mosquito to the vertebrate host. Mice vaccinated with yeast-produced Pvs25 adsorbed to alum (aluminium hydroxide) produced antisera that, when ingested with *P. vivax*-infected chimpanzee blood, completely inhibited the development of oocysts in mosquitoes (Hisaeda *et al.*, 2000).

Several murine monoclonal antibodies against recombinant Pvs25 have been produced and shown to possess transmission-blocking activity against mosquito-stage *P. vivax* parasites. In laboratory membrane-feeding experiments, the monoclonal antibody 2A8 blocks the transmission of *P. vivax* to mosquitoes from the blood of a *P. vivax*-infected chimpanzee and from the blood of patients with vivax malaria. Here, we report the preparation, crystallization and preliminary X-ray crystallographic studies of the complex of Pvs25 with the Fab fragment of 2A8. These structural studies will define the interaction between Pvs25 and the Fab frag-

ment of antibody 2A8 and may contribute to the understanding of how antibodies can block parasite development in the mosquito.

2. Methods

2.1. Preparation of Pvs25

Expression and purification of Pvs25 took place as described previously (Hisaeda *et al.*, 2000; Miles *et al.*, 2002). Briefly, the gene encoding Pvs25 from Ala23 to Leu195 from *Plasmodium vivax* genomic DNA (from Salvador I strain) was inserted into the yeast episomal plasmid YEpRPEU-3 and transformed into *S. cerevisiae* VK1 cells. The resulting cells were screened for the secretion of histidine-tagged protein. A positive colony was grown in a fermenter with recombinant protein production under the ethanol-inducible ADH2 promoter. The recombinant protein was purified using nickel-affinity, size-exclusion and hydrophobic interaction chromatography. N-terminal sequencing and electron-spray mass spectrometry confirmed the identity of the purified Pvs25 protein and its molecular weight of 20 502 Da. The purified protein contains 186 residues: five residues from the α-factor sequence (Glu-Ala-Glu-Ala-Ser), 173 residues of Pvs25 and eight residues from the affinity tag, Gly-Pro-His_6.

2.2. Preparation of Fab

The 2A8 antibody was produced on a large scale in mouse ascites fluid. IgG_1 was precipitated with 40% saturated ammonium sulfate and purified from the precipitate by ion-exchange chromatography on DEAE-Sepharose using an NaCl gradient. The IgG_1 was then cleaved with papain at an enzyme:antibody ratio (*w*:*w*) of 1:20 in 100 m*M* Tris–HCl, 150 m*M* NaCl, 2 m*M* mercaptoethanol, 2 m*M* NaEDTA pH 7.1 at 310 K for 4 h. Adding fresh iodoacetamide to a final concentration of 7.5 m*M* stopped the reaction. Fab was purified from the digestion mixture again by the use of DEAE-Sepharose chromatography. The Fab fractions were pooled and concentrated to obtain a final concentration of 6.4 mg ml^{-1} (0.138 m*M*) in 20 m*M* Tris–HCl pH 7.4.

2.3. Preparation of the Pvs25–Fab complex

When the purified Pvs25 (4.5 mg ml^{-1}, 0.219 m*M*) and Fab proteins were electrophoresed on a native gel, each migrated as a single band (see the leftmost two lanes of Fig. 1). When a mixture of Pvs25 and Fab was analyzed on a native gel, new bands appeared that were shifted in mobility (lane 1:1 in Fig. 1). In contrast to the proteins analyzed alone, the complex runs as three smeary bands. Possible reasons for this unusual behavior on a native gel could be that there is heterogeneity of overall charge in the complex or that some of the complex aggregates when in the gel. Using the native gel, we identified the ratio (*v*:*v*) of 1:3 (Pvs25:Fab) of our preparations of Pvs25 and of Fab that yielded the maximum amount of the complex (Fig. 1).

For the large-scale preparation of the complex, Pvs25 protein was mixed with Fab at a ratio of 1:3 (*v*:*v*) (Pvs25:Fab) and incubated at 310 K for 2 h. The resulting complex was purified by size-exclusion chromatography, which showed a single peak (Fig. 2) at an elution volume consistent with a molecular weight of 67 000 Da when compared with the elution volumes of molecular-weight standards run on the same column (not shown). Note that on the size-exclusion column there is no suggestion of aggregation in solution, as was suggested by the native gel (Fig. 1). The molecular weight of 67 000 Da indicates that the complex is composed of one Pvs25 molecule and one Fab molecule. The pooled fractions containing the Pvs25–Fab complex were concentrated using a 10 kDa molecular-weight cutoff centrifugal device.

2.4. Crystallization of the Pvs25–Fab complex

The Pvs25–Fab complex was concentrated to 8 mg ml^{-1} and buffer-exchanged to 20 m*M* Tris–HCl pH 7.4 for crystallization experiments. The initial crystallization conditions were found using Crystal Screens I and II and PEG/LiCl kits (Hampton Research). All crystallization experiments were performed at 293 K by the hanging-drop vapor-diffusion method. In each trial, 1 µl Pvs25–Fab complex protein was mixed 1 µl with precipitant solution and equilibrated as a hanging drop against a reservoir containing 500 µl precipitant solution. The Pvs25–Fab complex crystals were grown over a reservoir containing 20–25%(*w*/*v*) polyethylene glycol (PEG) 6000, 1 *M* LiCl, 100 m*M* citric acid pH 5.0. When hanging drops of Pvs25 alone, Fab alone and Pvs25–Fab complex were equilibrated in parallel over the same reservoir, crystals only formed in the drop containing the complex.

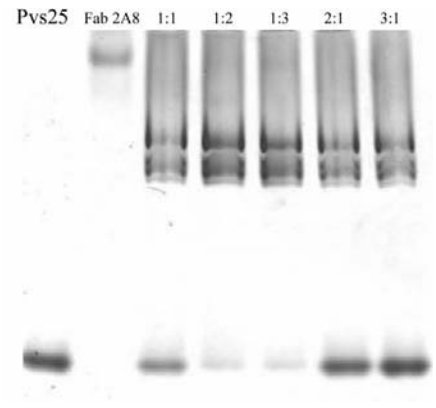

Figure 1
Native-gel analysis of Pvs25 alone, Fab2A8 alone and mixtures of Pvs25 and Fab (Pvs25:Fab) at five different ratios (*v*:*v*). The complex runs as three smeared bands. A Tris–glycine gel of 4–20% acrylamide was used. We used the 1:3 ratio for the formation of the Pvs25–Fab complex that was crystallized.

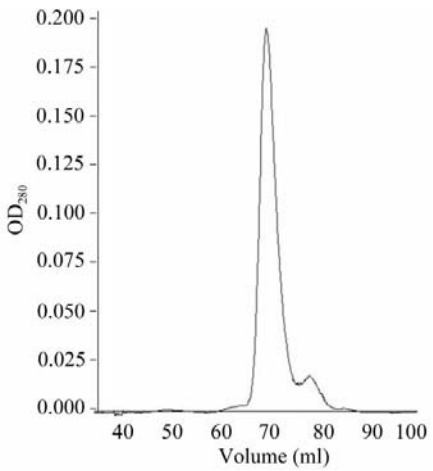

Figure 2
Elution profile of the Pvs25–Fab complex by size-exclusion chromatography using a Superdex 75 16 × 60 column running in 50 m*M* Tris–HCl, 150 m*M* NaCl pH 7.5. The large peak extending to about 0.2 OD_{280} is the Pvs25–Fab complex. The smaller peak at its base is unbound Fab protein.

Figure 3
Monoclinic crystals of the Pvs25–Fab complex. The crystals grew as clusters of rectangular bars with typical dimensions of 0.2 × 0.15 × 0.07 mm.

Table 1
X-ray data-collection statistics.

Values in parentheses are for the last resolution shell.

	Native *A*	Native *B*
Resolution (Å)	50.0–3.50 (3.56–3.50)	40.0–4.00 (4.07–4.00)
X-ray source	22-ID (APS)	22-ID (APS)
Wavelength (Å)	0.97942	1.0
Space group	$P2_1$	$P2_1$
Unit-cell parameters		
a (Å)	86.3	86.8
b (Å)	61.7	61.0
c (Å)	142.7	149.3
β (°)	101.7	104.3
Reflections observed	84192	72628
Unique reflections	18476 (866)	13115 (665)
Completeness (%)	96.3 (89.9)	98.6 (97.5)
Redundancy	4.6	5.5
$R_{\rm merge}$† (%)	25.0 (65.0)	19.2 (58.7)
Average $I/\sigma(I)$	6.0 (2.3)	8.6 (2.2)

† $R_{\rm merge} = \sum_h \sum_i |I_{h,i} - \langle I_h\rangle| / \sum_h \sum_i |I_{h,i}|$, where $I_{h,i}$ is the ith intensity measurement of reflection h and $\langle I_h\rangle$ is the average intensity of that reflection.

Crystals have been observed to form in identical drops of Pvs25 alone (Saxena *et al.*, 2004) and of Fab alone, but at different conditions and not under the conditions under which the Pvs25–Fab complex crystallized. The Pvs25–Fab crystals usually appeared after 7–8 d and grew to maximum dimensions of 0.2 × 0.15 × 0.07 mm. The crystals usually grow as clusters as shown in Fig. 3, but single crystals are readily obtained by lightly touching a cryoloop to the surface of a cluster.

3. Results and discussion

For data collection, Pvs25–Fab complex crystals were transferred into a solution identical to the growth conditions but with a higher PEG concentration of 30%(*w*/*v*) for cryoprotection and flash-frozen by plunging directly in liquid nitrogen. Two crystals yielded X-ray data sets (native *A* and native *B*) that were collected at 100 K at beamline 22-ID at Argonne National Laboratory (APS). Indexing, integration, scaling and merging of the data were carried out using the *HKL*2000 software package (Otwinowski & Minor, 1997). $F_{\rm obs}$ values were produced using the program *TRUNCATE* from the *CCP*4 suite of programs (Collaborative Computational Project, Number 4, 1994). Data-collection and processing statistics are given in Table 1 and in Supplementary Table 1[1].

In attempts to improve the quality of the Pvs25–Fab crystals, the nature and concentration of the precipitant were varied, the protein concentration was changed and the addition of various salts and additives was tried. Macroseeding by the introduction of a small crystal into a crystallization drop was not fruitful. Co-crystallization with various heavy-metal compounds was performed both to obtain derivatives and to improve the crystals. Crystals grew but they were little improved.

The Matthews coefficient based on two complexes in the asymmetric unit for the native *A* data set is 2.78 Å^3 Da^{-1}, consistent with a solvent content of 56%. For the native *B* data set, $V_{\rm M}$ was 2.86 Å^3 Da^{-1}, consistent with a solvent content of 57%. These $V_{\rm M}$ values lie within the range usually observed in protein crystals (Matthews, 1968) and are in line with two complexes per asymmetric unit as indicated by the self-rotation function and molecular-replacement results.

The self-rotation function calculated with *POLARRFN* (Collaborative Computational Project, Number 4, 1994) shows a substantial peak on the $\kappa = 180°$ section that is 80% of the height of the origin peak (Fig. 4). This peak is consistent with the existence of twofold non-crystallographic symmetry in the asymmetric unit. Initial molecular-replacement calculations using the program *BEAST* (Read, 2001) located the two Fab molecules in native data sets *A* and *B* using the 2E8 Fab (Trakhanov *et al.*, 1999; PDB code 12e8) as a search model. Using the calculated structure factors from the positioned 2E8 Fab molecules in a $2F_{\rm o} - F_{\rm c}$ map, preliminary electron density for the Pvs25 protein was observed in the antigen-binding region of the 2A8 Fab. This electron density confirms that both the Pvs25 and the Fab molecules are indeed present in the crystal; this had been difficult to confirm by SDS–PAGE. Attempts are being made to improve this electron density using the non-crystallographic symmetry, by inter-crystal density averaging and by attempting to obtain crystals that diffract to higher resolution. Model building and refinement are in progress in order to reveal the structure of the Pvs25–Fab complex from these X-ray data.

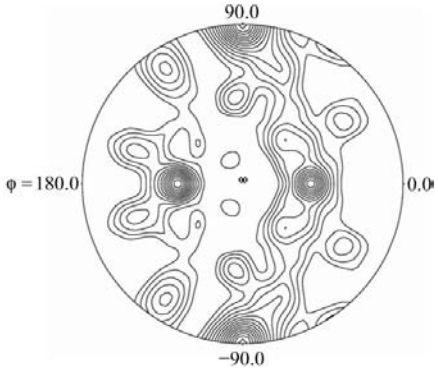

Figure 4
Self-rotation function using the Pvs25–Fab complex data. The $\kappa = 180°$ section is shown from a self-rotation function calculated with all data in the range 40–5.0 Å and a 34 Å radius of integration. Note the strong peak at $\omega = 46$, $\varphi = 0°$ and, equivalently, at $\omega = 134$, $\varphi = 180°$.

[1] Supplementary material has been deposited in the IUCr electronic archive (Reference: ZA5072). Details for accessing these data are described at the back of the journal.

We thank the members of the Structural Biology Section for discussions and members of the Malaria Vaccine Development Branch for supplying purified Pvs25 protein. Data were collected at Southeast Regional Collaborative Access Team (SERCAT) 22-ID beamline at the Advanced Photon Source of the Argonne National Laboratory. Supporting institutions may be found at http://www.ser-cat.org/members.html. Use of the Advanced Photon Source was supported by the US Department of Energy, Office of Science, Office of Basic Energy Sciences under Contract No. W-31-109-Eng-38.

References

Brünger, A. T., Adams, P. D., Clore, G. M., DeLano, W. L., Gros, P., Grosse-Kunstleve, R. W., Jiang, J.-S., Kuszewski, J., Nilges, M., Pannu, N. S., Read, R. J., Rice, L. M., Simonson, T. & Warren, G. L. (1998). *Acta Cryst.* D**54**, 905–921.

Collaborative Computational Project, Number 4 (1994). *Acta Cryst.* D**50**, 760–763.

Hisaeda, H., Stowers, A. W., Tsuboi, T., Collins, W. E., Sattabongkot, J. S., Suwanabun, N., Torii, M. & Kaslow, D. C. (2000). *Infect. Immun.* **68**, 6618–6623.

Kaslow, D. C., Quakyi, I. A., Syin, C., Raum, M. G., Keister, D. B., Coligan, J. E., McCutchan, T. F. & Miller, L. H. (1988). *Nature (London)*, **333**, 74–76.

Matthews, B. W. (1968). *J. Mol. Biol.* **33**, 491–497.

Mendis, K., Sina, B. J., Marchesini, P. & Carter, R. (2001). *Am. J. Trop. Med. Hyg.* **64**, 97–106.
Miles, A. P., Zhang, Y., Saul, A. & Stowers, A. W. (2002). *Protein Expr. Purif.* **25**, 87–96.
Otwinowski, Z. & Minor, W. (1997). *Methods Enzymol.* **276**, 307–326.
Read, R. J. (2001). *Acta Cryst.* D**57**, 1373–1382.
Saxena, A. K., Saul, A. & Garboczi, D. N. (2004). *Acta Cryst.* D**60**, 706–708.
Stowers, A. & Carter, R. (2001). *Exp. Opin. Biol. Ther.* **1**, 619–628.
Tachibana, M., Tsuboi, T., Templeton, T. J., Kaneko, O. & Torii, M. (2001). *Mol. Biochem. Parasitol.* **113**, 341–344.
Trakhanov, S., Parkin, S., Raffai, R. Milne, R., Newhouse, Y. M., Weisgraber, K. H. & Rupp, B. (1999). *Acta Cryst.* D**55**, 122–128.
Tsuboi, T., Kaslow, D. C., Gozar, M. M., Tachibana, M., Cao, Y. M. & Torii, M. (1998). *Mol. Med.* **4**, 772–782.